Engineering and Technology Journal
Journal homepage: https://etj.uotechnology.edu.iq

SDR-based Intelligent Cooperative Spectrum Sensing for Cognitive Radio Systems

Ali A. Radhi[a], **Hanan A. R. Akkar**[a*], **Hikmat N. Abdullah**[b]

[a] Electrical Engineering Engineering Dept., University of Technology-Iraq, Alsina'a street, 10066 Baghdad, Iraq.
[b] Information and Communication Engineering Dept., University of Al-Nahrain, Baghdad, Iraq.
*Corresponding author Email: alimsc@uomustansiriyah.edu.iq

HIGHLIGHTS

- The real-time sensing performance of the new intelligent cooperative spectrum sensing based on the denoised mixed feature method paired with K-Medoids is verified.
- Two RTL-SDR hardware receivers, a host laptop computer, and a USRP-SDR hardware transmitter are used.
- The theoretical and practical sensing performance validity of the developed scheme is confirmed based on the SDR platform.

ARTICLE INFO

Handling editor: Ivan A. Hashim

Keywords:
Software-Defined Radio; RTL-SDR; USRP-SDR; GNU-Radio; Denoised Mixed Features.

ABSTRACT

In this paper, the software and hardware of a software-defined radio (SDR) platform are used to implement and verify the blind real-time sensing act of intelligent collaborative spectrum sensing based on a new theoretical formula for constructing denoised mixed features named MSKU3 and paired with an unsupervised machine learning K-Medoids algorithm. Two low-cost RTL-SDR dongle hardware receivers are used as two cooperative unlicensed secondary users to capture the radio frequency of a licensed primary user channel. A host personal computer is used as a fusion center to run GNU-Radio software signal processing blocks to implement the developed method, and a single Universal Software Radio Peripheral (USRP) N210 hardware transmitter based on FPGA is used to take up unoccupied desired radio frequency bandwidth. Two scenarios of signal-to-noise ratio levels have been adopted to verify and test the sensing performance of the developed system. The first one occurs when unlicensed secondary users have equal signal-to-noise ratio values. The second occurs when unlicensed secondary users have different signal-to-noise ratio values since each secondary user has their location. The experimental results of detecting action in terms of the probability of detection for the proposed method show that the theoretical and practical results are very close to each other.

1. Introduction

The enormous increase in the number of mobile devices, combined with the stationary handling of frequency bands, has resulted in a lack of accessible available bandwidth [1]. According to the findings of a study conducted by the Federal Communication Commission (FCC), the percentage of licensing spectrum that is being continuously utilized by the licensed Primary User (PU) is lower than thirty percent [2]. According to FCC reports, there are bandwidth vacancies, particularly in the TV band, sometimes known as TV white space (TVWS) [3]. Cognitive Radio (CR) is a telecommunication technique employed to address the issue of bandwidth shortages [4]. To exploit the bandwidth usage, in CR, an unlicensed Secondary User (SU) utilizes the licensed bandwidth of PU [5]. To avoid interference with PU bandwidth, Spectrum Sensing (SS) is a crucial task in CR networks that keep an eye on the licensing frequency band to identify the status of the PU and distinguish the locations of bandwidth holes [6].

In the academic literature, there are a variety of traditional narrowband SS feature detection algorithms that have been proposed. These algorithms are used to determine the state (occupied or unoccupied) of a PU in a certain frequency band. Some examples of these techniques include: energy detection (ED) [7], Cyclostationary Features (CFs) Detection [8], eigenvalue of the covariance matrix (CM) of random matrix theory (RMT)-based detection methods [9–11], and information geometry theory (IGT)-based methods [12]. Consequently, previous classical SS techniques are unable to adapt to the dynamic nature of the actual channel because they rely on a fixed detection threshold [13]. Lately, many Cooperative Spectrum Sensing (CSS) schemes based on machine learning (ML) and deep learning (DL) approaches combined with classical features methods of RMT have been proposed. They extract energy features (EFs) of RMT for sensing samples of SU, which are based on

http://doi.org/10.30684/etj.2023.136258.1306
Received 07 October 2022; Accepted 05 January 2023; Available online 24 January 2023
2412-0758/University of Technology-Iraq, Baghdad, Iraq

second-order moments, to train ML algorithms [14–17]. Unfortunately, all of the ML and DL-based CSS approaches that are based on EFs are more vulnerable to noise variations and perform poorly at low signal-to-noise ratios (SNR) [18–20]. As a result, previous CSS schemes had numerous issues, such as a high degree of overlapping between ML groups, improper categorization of desired features, and weak detecting performance [21].

In recent work published in [22,23], we provide a new blind intelligent CSS built on new denoised mixed features (DMFs) techniques and combined with unsupervised ML algorithms. We prove that the unsupervised ML-based CSS schemes that use denoised features (DFs) generated by high-order moments such as the Jarque-Bera (JB) formula or Skewness (Sk) and access Kurtosis (Ku-3) have less computational complexity and are more immune to noise fluctuation at low SNR. In [22], we established four novel denoised features (DFs) methods using the Jarque-Bera (JB) formula to improve the clustering of unsupervised ML algorithms (K-Means) and the sensing performance of CSS schemes. Similarly, in [23], we developed two new DMF methods using third and fourth moments such as Sk and Ku-3, respectively, to boost the classification process of unsupervised ML algorithms (K-Medoids) and enhance the detection performance of CSS schemes in terms of Probability of Detection (Pd).

To verify and implement the real-time detecting operation of the CSS scheme based on developed DMF methods, we use the Software Defined Radio (SDR) platform and select the maximum values of Sk and Ku-3 of the DMF vectors (MSKU3) [23] method as characteristic features for receiving sensed samples of SU. SDR has served as the cornerstone for the development of the SS methods. It is feasible to incorporate the SS techniques into communication equipment that is also adaptable and user-defined. SDR is a technique that implements communication capabilities with software operating on adaptable hardware [24,25]. In the literature, different studies have provided real-functioning implementations of SS methods using SDR. In the literature [26], one of the most widely used pieces of SDR hardware is the Universal Software Radio Peripheral (USRP), which is used to implement energy feature-based SS. The researchers of these publications evaluated the practical sensing performance of an EFs realization based on USRP hardware for their theoretical performance and discussed their findings. The paper [27,28]described the real-time realization of the SS method based on the covariance matrix of RMT employing USRP SDR hardware. In [29], a real-time adaptive SS method using EFs and CFs was realized by applying the USRP hardware platform and the GNU-Radio software throughout Rayleigh fading. Some of the studies on the development of SS make use of costly SDRs like USRP. However, some of the more recent work makes use of ultra-low-cost SDRs like RTL-SDR hardware. In the literature [30]. The author utilized SDR platforms such as RTL-SDR and GNU-Radio software-based IoT to implement real-time SS exploiting EFs. The literature [31] implements real-time sensing performance of the SS method based on EFs employing RTL-SDR as the receiver. In this work, we use GNU-Radio as a software toolkit to implement the actual-time detecting performance of the MSKU3 method-based CSS scheme [23], carrying on hardware made up of an RTL-SDR receiver and a USRP transmitter. In GNU-Radio Companion, a signal capture application is created, and samples collected are evaluated afterward to assess sensing accuracy. We explore the practical actual-time sensing act of a spectral domain of the MSKU3 method-based CSS scheme and compare it with its theoretical sensing performance. Based on our review of the relevant literature, we can confidently say that this is the first time the frequency domain MSKU3 method-based CSS scheme has been implemented and analyzed using SDR.

Our novel contributions presented in this article are the following: Contributions [29,32].

1) Theoretical and practical real-time sensing performance analysis of a new denoised mixed-feature MSKU3 method-based CSS scheme in a real-channel environment have been performed.
2) The characteristics of implementing an MSKU3 method-based CSS scheme using RTL-SDR hardware, GNU-Radio software, and USR hardware is described in detail.
3) The practical detecting capability of the MSKU3 approach is validated using two scenarios: first, the two cooperative RTL-SDR receivers collect detected signals with the same SNR; second, each RTL-SDR receiver gathers up the signals with a different SNR since it is located in a separate location.

The other sections of the paper are ordered as follows. The theory behind MSKU3 method-based cooperative spectrum sensing is described in Section 2. Section 3 provides details on the software model and hardware setup. The test results and associated analysis are provided in Section 4. The conclusion is given in Section 5.

2. Cooperative Spectrum Sensing Framework

In the CSS scheme of CR, there are two hypotheses, as shown in Equation (1), that could be used to describe the signal that SU has captured [33] :

$$\begin{aligned} \mathcal{H}_0 &: \mathrm{x_i(j)} = \mathrm{w_i(j)} \\ \mathcal{H}_1 &: \mathrm{x_i(j)} = \mathrm{h_i(j)s(j)} + \mathrm{w_i(j)} \end{aligned} \tag{1}$$

Where *i* and j represent the indices of the number of SU and received samples in the CSS scheme, respectively. The null hypothesis, H_0, is a channel with additive white Gaussian noise (AWGN) $w_i(j)$ signal, and no PU s(j) signal. The alternative hypothesis, H_1, is a channel with noise $w_i(j) \sim \mathcal{N}(0, \sigma_w^2)$ signal plus PU $s(j) \sim \mathcal{N}(0, \sigma_s^2)$ signal. Here, $h_i(j)$ is the channel gain between the PU signal and *i*th SU_i, which is proposed here as $h_i(j) = 1$ under no fading channel condition. Consequently, the complex samples of captured $x_i(j)$ signal which are detected by each SU, $X = [\, x_1, x_{2,\ldots,} x_M]^T$, can be described by the following Equation (2) [33]:

$$X = \begin{bmatrix} x_1 \\ x_2 \\ \vdots \\ x_M \end{bmatrix} = \begin{bmatrix} x_1(1) & x_1(2) & \cdots & x_1(N) \\ x_2(1) & x_2(2) & \cdots & x_2(N) \\ \vdots & \vdots & \ddots & \vdots \\ x_M(1) & x_M(2) & \cdots & x_M(N) \end{bmatrix} \quad (2)$$

Where $\in \mathbb{C}^{M \times N}$, and T stands to a transposition operator.

Two commonly used parameters to assess the detecting performance of CSS schemes are P_d and the probability of false alarm (P_f). P_D is the possibility of choosing which frequency to active when a signal is already being sent out by the PU as written in Equation (3) [34].

$$P_d = P[\mathcal{H}_1 \mid \mathcal{H}_1] \quad (3)$$

P_F is the possibility of deciding the frequency to be active when in actuality it is not, as written in Equation (4) [34].

$$P_f = P[\mathcal{H}_1 \mid \mathcal{H}_0] \quad (4)$$

According to the IEEE 802.22 standard, P_D should be equal to or greater than 0.9 and P_F should be equal to or less than 0.1 as small as possible at SNR equal to -20dB so that underused wireless channels can be avoided [35].

2.1 Denoised Mixed Feature method – based Cooperative Spectrum Sensing

The theoretical analysis of a novel DMFs method-based CSS scheme is introduced in [23]. As shown in Figure 1 a new CSS scheme based on the DMF method MSKU3 consists of one PU signal on/off licensed channel, several SUs, and one fusion center (FC) unit.

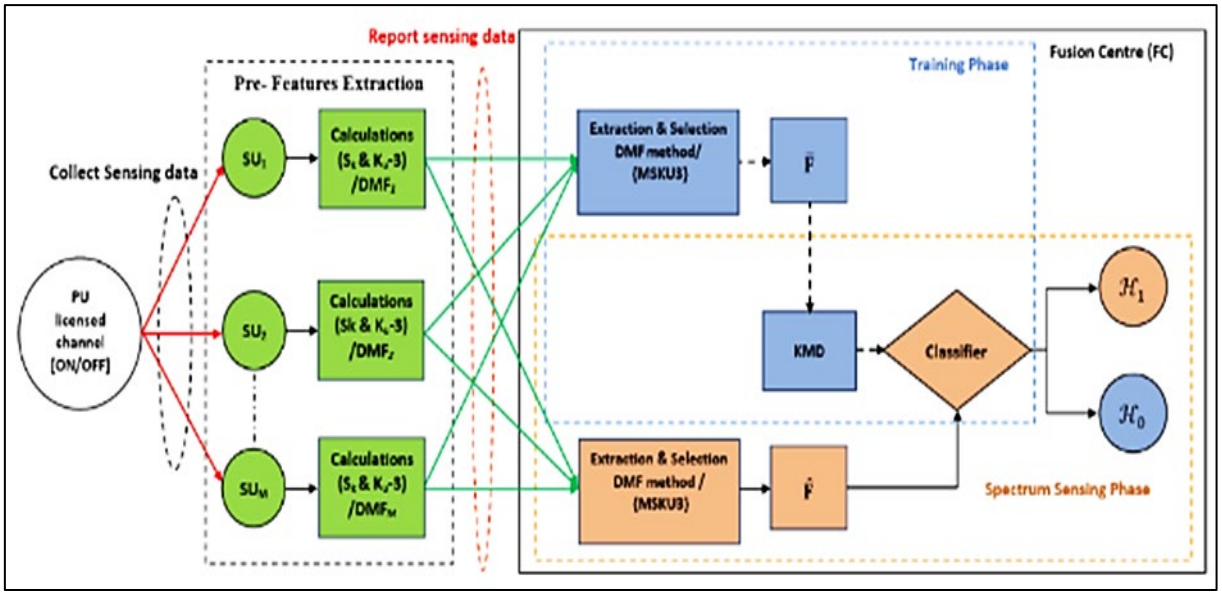

Figure 1: The MSKU3 method and KMD algorithm-based CSS scheme [23]

All SUs in the developed scheme is responsible for sensing the status of the PU signal if it is active or idle on the licensed channel. Then, collecting an adequate number of sensed samples of PU signal by each SU_i to construct the $x_i(j)=[x_i(1), x_i(2),\ldots, x_i(N)]$ vector. After that, in the "Pre-Features Extraction" section, the formula of 3rd and 4th high-order moments Sk and Ku-3, respectively, are employed to calculate the statistics of the collected vector $x_i(j)$ for each SU according to the following Equation (5) and Equation (6) [36] :

$$S_k(x_i) = \frac{E[(x_i - E[x_i])^3]}{E[(x_i - E[x_i])^2]^{\frac{3}{2}}} = \frac{\frac{1}{N}\sum_{j=1}^{N}(x_{ij} - \bar{x}_i)^3}{\left[\frac{1}{N}\sum_{j=1}^{N}(x_{ij} - \bar{x}_i)^2\right]^{\frac{3}{2}}} \quad (5)$$

$$K_u(x_i) - 3 = \frac{E[(x_i - E[x_i])^4]}{E[(x_i - E[x_i])^2]^2} - 3 = \frac{\frac{1}{N}\sum_{j=1}^{N}(x_{ij} - \bar{x}_i)^4}{\left[\frac{1}{N}\sum_{j=1}^{N}(x_{ij} - \bar{x}_i)^2\right]^2} - 3 \quad (6)$$

Ku (x_i)-3 of each SU_i node are combined by a new formula as written in Equation (7) to generate a new DMF_i for each SU_i [23].

$$\text{The} \qquad R(x_i - 3) \quad = \sqrt{[S_k(x_i)^2 + (K_u(x_i) - 3)^2]} \tag{7}$$

Here, $R(x_i - 3)$ represents the DMF_i of *i*th SU_i which is transmitted into the FC unit to construct the DMF-vector as expressed in Equation (8) [23] :

$$R(x_i - 3) \quad = [R(x_1 - 3) \ , R(x_2 - 3) \ , \dots , R(x_M - 3) \ ]^T \tag{8}$$

In the FC unit, the following newly developed formula, Equation (9), is applied to Equation (8) to obtain the maximum statistical value of the DMF-vector [23] :

$$F_{MSKU3} = \frac{1}{M} \underset{1 \le i \le M}{max} R(x_i - 3) \tag{9}$$

Here, the capital symbol F is an abbreviation of the word "Feature" and the subscript MSKU3 refers to the type of denoising mixed feature method that is used. According to the new DMF method, a training set of feature vector $\bar{F}$, $\bar{F} = \{F^1_{MSKU3}, F^2_{MSKU3}, \dots , F^l_{MSKU3}\}$ are employed to teach the unsupervised ML KMD approach to establish a classifier based on (H0, H1) conditions of PU signal.

3. The SDR Hardware and Software Requirements

In this part, the real-time perception performance of a new intelligent CSS based on a novel MSKU3 method is confirmed, and the key parts that are used to test the real-time sensing performance of the developed scheme are described.

3.1 The SDR Hardware Specifications

The important SDR hardware parts that are chosen and used to design and test the real-time sensing performance of the proposed scheme (MSKU3-based CSS) are shown in Figure 2. They are coming with several pieces of hardware, such as the RTL-SDR USB dongle, the Universal Software Radio Peripheral (USRP®) from Ettus Research, and a laptop personal computer (PC) running the GNU-Radio Companion (GRC) software.

(a): RTL-SDR USB dongle **(b): Laptop personal computer** **(c): USRP-SDR**

Figure 2: The essential adopted SDR hardware components for MSKU3-based CSS, (a): RTL-SDR USB dongle,(b): Laptop personal computer, (c): USRP-SDR

3.1.1 RTL-SDR hardware

As can be seen in Figure2 (a), the omni-directional antenna that is included with the RTL-SDR USB dongle functions as a wireless receiver. This receiver makes use of the Realtek RTL 2832U chip, which has a radio frequency (RF) range of 24 MHz to 1,766 MHz, a bandwidth of 3.2 MHz, and an analog-to-digital converter (ADC) resolution of 8 bits. The RTL-SDR hardware is capable of receiving FM radio, UHF band signals, ISM signals, GSM, 3G, and LTE mobile radio, GPS, and satellite signals, as well as any information that the designer can (lawfully) send.

3.1.2 Universal Software Radio Peripheral hardware

On the other hand, as can be seen in Figure2 (c), Ettus Research's USRP® hardware family consists of configurable FPGA with transmit and receive (Tx and Rx) SDR capabilities. One of the members of the USRP® family is the USRP® N210. The USRP N210 is capable of processing signals with both a large bandwidth and a wide dynamic range frequency. The USRP N210 is made with a Xilinx Spartan® 3A-DSP 3400 FPGA, 100 MS/s dual ADC, 400 MS/s dual DAC, 6GHz bandwidth, and a Gigabit Ethernet connection to make it easier for information to go to and from the PC.

3.1.3 Personal computer

Furthermore, as shown in Figure 2 (b), a PC, which is equipped with an Intel Core i5-8250U, 16GB of RAM, and 1TB of hard drive space, is used to run GRC software to program the SDR boards to act as a specific type of radio and to store and display information.

3.2 The SDR Software Requirements

Besides that, the GRC serves as a framework for developing the software blocks of receivers and transmitters of the developed scheme. In addition to make it possible to develop new function blocks, GRC makes it feasible to handle discontinuous signals by mixing a variety of functional blocks [37]. Figure 3 displays a snapshot of the experimental equipment.

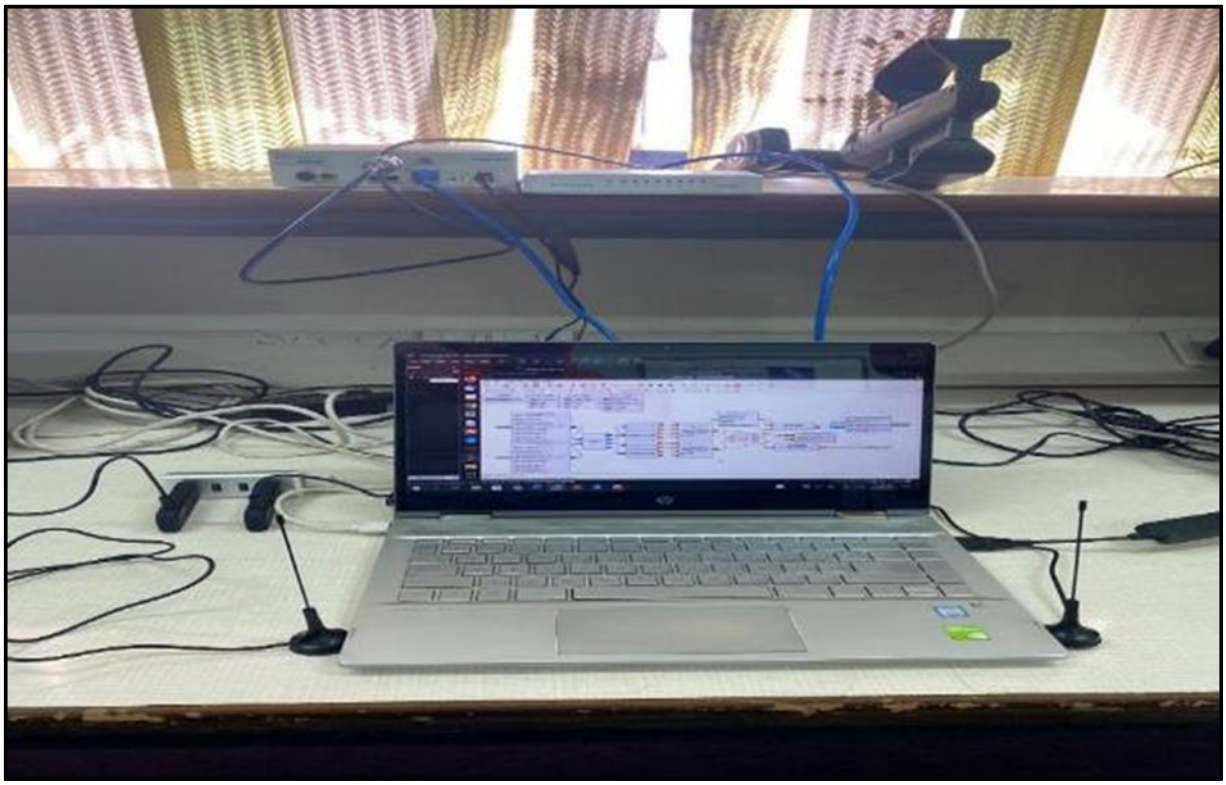

Figure 3: The snapshot of the real experimental setup implementation of MSKU3-based CSS

3.3 Experimental Setup

On the receiving side, one of two RTL-SDR receivers is allocated to each SU and connected to the PC through a USB port in order to accomplish the sensing performance of the developed method. In our experiment, RTL-SDRs work together to sample and digitize PU's RF signals that are sent between 25 MHz and 1.75 [37,38] Here, the PC acts as a ring link between the transmitter side and the receiver side and works as an FC unit. The PC is using a virtual machine (VMware® Workstation 16 Pro) to run GRC software version 3.8.1.0 based on the operating system (Ubuntu 20.04 LTS). The GRC is software that provides input/output blocks and enables the implementation of the DSP blocks and SDR algorithms of the proposed method, which is presented in experiment [39]. On the transmitting side, a single USRP N210-SDR transmitter is connected to a PC via Gigabit Ethernet. It is used to take up an empty PU RF channel as decided by the FC unit.

Figure 4 shows the experimental setup of the GNU radio block diagram software for the entire developed scheme, which includes the transmitting side, the new denoised mixed feature method, and the receiving side. Each RTL-SDR Source GNU Radio block provides the python software codes to interface between GRC and RTL-SDR hardware. The GNU Radio RTL-SDR Source block software is used to set up important tuning parameters like carrier frequency fc and sample rate fs (bandwidth) so that the antenna and RTL-SDR dongle can pick up the desired PU RF signals from the actual channel. The fc is set to any frequency in the coverage range of the RTL-SDR antenna by the "Ch0" parameter, and the "Sample Rate" parameter sets the fs to 2 MHz.The multiplexer block controls the connection of two RTL-SDR hardware sources between the training and sensing stages. Once the training process is done, the sensing stage is activated to accomplish sensing operation, and vice versa. The training and sensing blocks are equivalent. They contain the essential Python codes to perform all the theoretical equations of the developed scheme. Following the KMD algorithm, the optimal classifier block based on two optimum medians of PU conditions is constructed (H0, H1). The role of the classifier block is to enable or disable the USRP-SDR hardware transmitter according to the PU RF channel. If a PU RF signal is present (H1), the classifier disables transmission of USRP-SDR hardware. If there is no PU RF signal (H0), the classifier lets the USRP-SDR transmitter use an empty channel. On the receiver side, the USRP-SDR Sink block provides the FPGA software codes to interface between GRC and the USRP N210 -SDR hardware transmitter. The USRP N210 -SDR hardware transmitter employed to occupy an unoccupied PU RF channel.

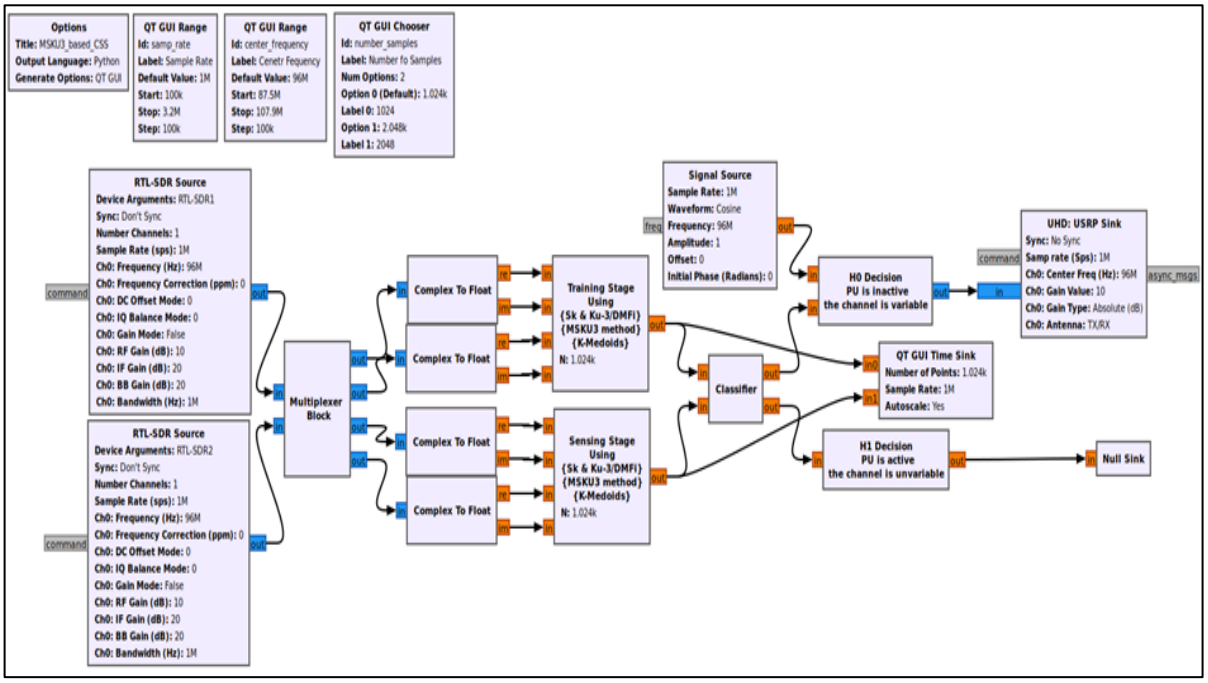

Figure 4: The GNU-Radio block diagram of MSKU3-based CSS scheme

4. Results and Discussion

In this part, the practical sensing performance of the developed method-based CSS system in a real-channel environment is confirmed. In addition, a comparison between the practical and theoretical measurements of the developed method (MSKU3)-based CSS scheme with different SNR conditions has been performed.

4.1 Performance Evaluation of The MSKU3-Based CSS Scheme in The Real Channel

To further verify the effectiveness of the real-time sensing performance of the newly developed DMF method (MSKU3)-based CSS scheme in a more challenging wireless communication environment, the indoor real-channel environment has been selected. The indoor channel measurements are performed within the lab room on the middle floor of the communication research center in the Ministry of Science and Technology in Baghdad, Iraq (latitude 33° 16' 49" North, longitude 44° 23' 15" East, altitude 15 m), as depicted in Figure 5.

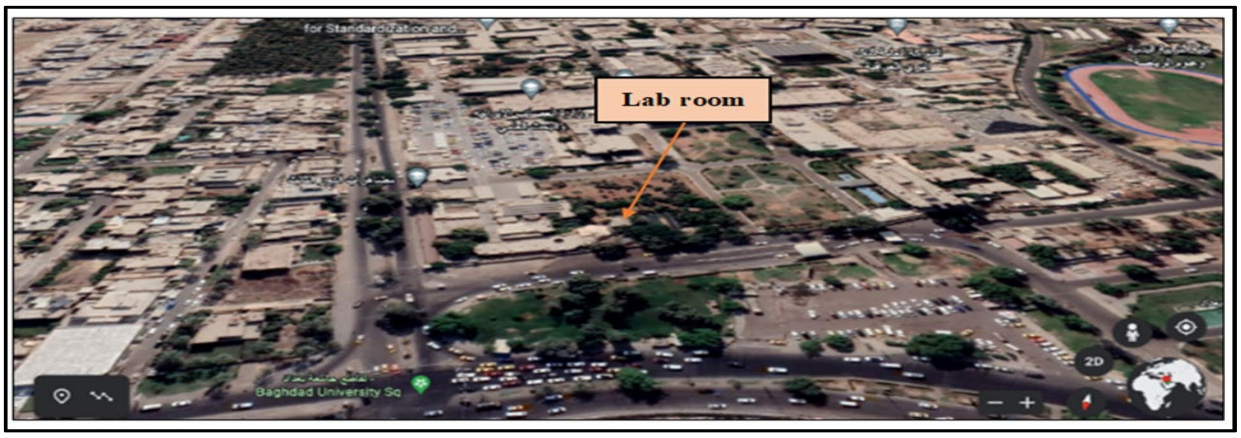

Figure 5: The indoor measurement has taken place inside the Ministry of Science and Technology

The chosen site room is a challenge for our developed framework because it has walls, floors, and other surfaces that reflect electromagnetic waveforms. These surfaces introduce the complex patterns of a wireless indoor environment, such as RF interference, degradation, fluctuation, and variation against the RF of the PU signals [40]. The real-time activities of the occupied and unoccupied (holes) portions of the RF bandwidth of the PU from 25 MHz to 1.766 GHz are recorded by the spectrum analyzer device Tek RSA6100A as shown in Figure 6. Then, during sensing operation, the tuning frequency fc of both RTL-SDR receivers is set to any frequency between 24 MHz and 1,766 MHz, which is the RF range that the RTL-SDR device bandwidth can cover, and the sample rate fs is set to 2 MHz, while the USRP N210-SDR hardware transmitter utilizes the frequency fc of the unoccupied channel (hole) to broadcast a test signal, as illustrated in Figure 7.

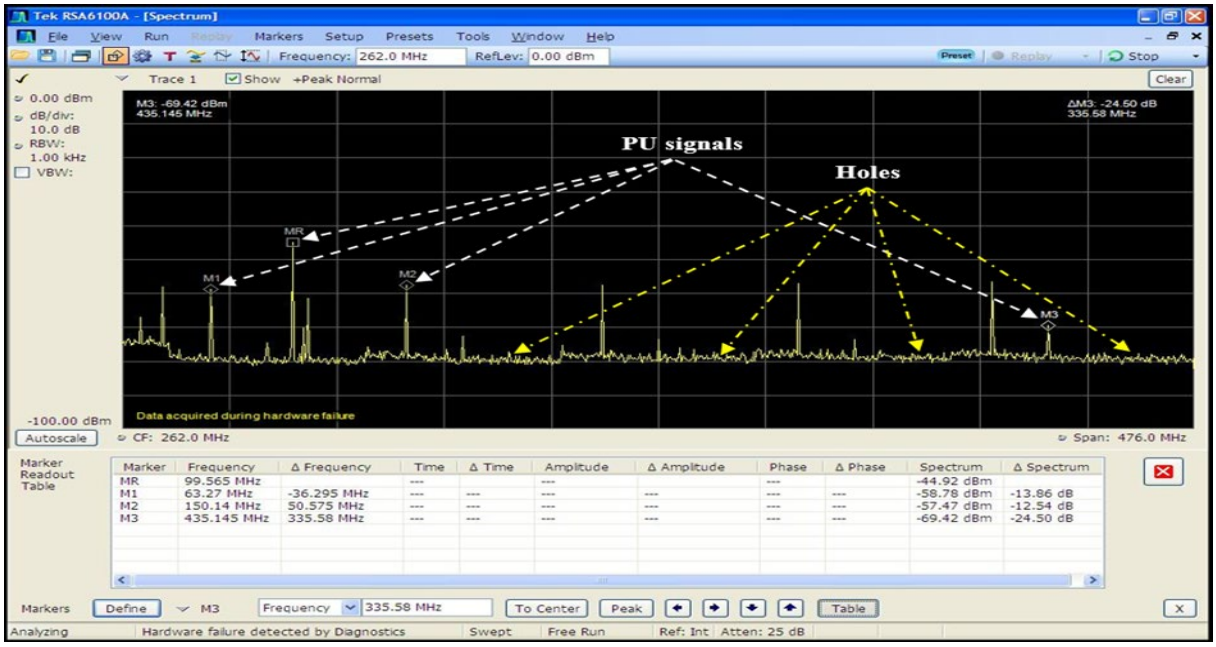

Figure 6: The real RF bandwidth of the PU from 25 MHz to 1.766 GHz, recorded by the spectrum analyzer Tek RSA6100A

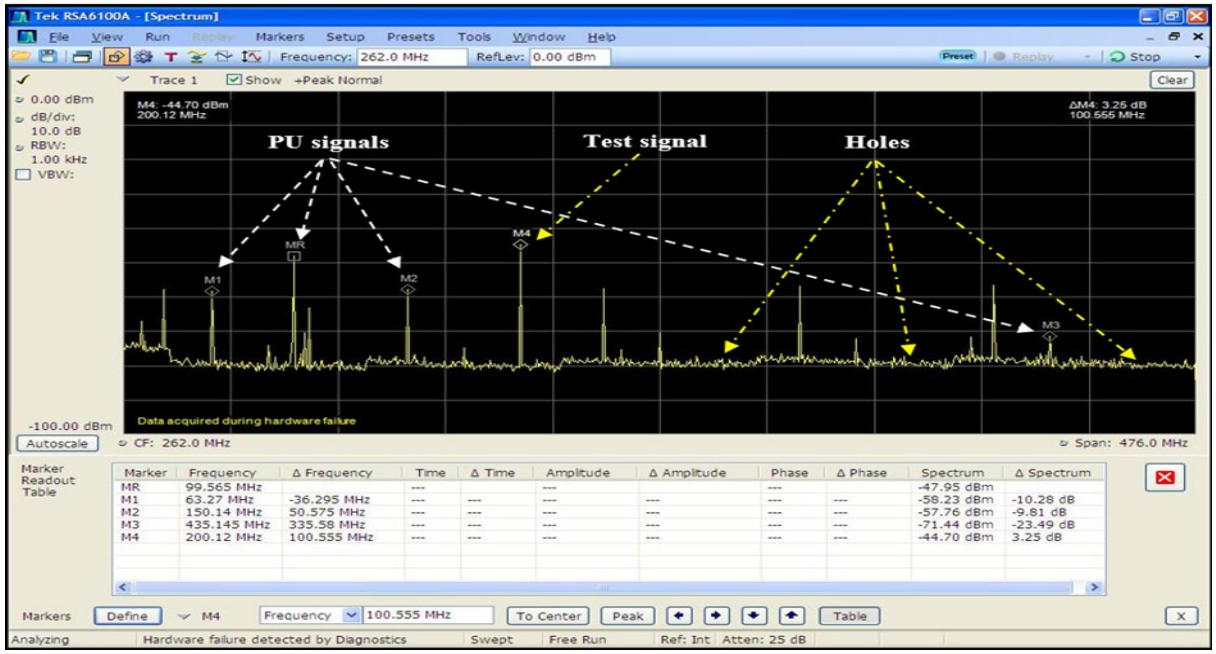

Figure 7: The detection and utilization of the unoccupied RF channel (hole) using a test signal

The real recorded measurements of RF ranging from 25 MHz to 1.6777 GHz for the indoor site channel when the noise floor is about -80 dBm are presented in Table 1. It contains the probability of detection (Pd) of the sensed frequency fc for each active PU signal and hole.

Then, based on the results of Pd in Table 1, the average probability of detecting the MSKU3-based CSS scheme in an indoor channel is 0.96 dBm. As a result, the practical measurements support the theoretical aspect of the developed method and confirm its sensing capability in an actual environment.

Table 1: The Pd of the MSKU3 method with various sensed frequencies in the indoor channel

Sensed frequency (MHz)	Probability of detection (Pd)	SNR (dBm)	Status	Utilization
63.27	0.95	-58.23	Occupied	No
99.565	0.97	-47.95	Occupied	No
150.14	0.95	-57.76	Occupied	No
200.12	0.99	-44.70	Unoccupied	Yes
435.145	0.94	-71.44	Occupied	No

4.2 Comparison of The Theoretical and Practical Measurements of The MSKU3 Method

This part compares the practical and theoretical measurements and the extent of their affinity for the developed MSKU3 method-based CSS scheme in a real environment. Figure 8 and Table 2 show the all theoretical and practical experimental findings of the receiver operation characteristics (ROC) curves for the MSKU3-based CSS method in parameters of Pd and Pf when using RTL-SDR receivers at various SNR values. As can be seen from Figure 8 (a) and the second column of Table 2, when the practical components are adjusted to N = 1000 samples, M = 2 SUs, Pf = 0.1, and at SNR = [-16dB, -16dB], there is a convergence between the theoretical and practical performances of CSS based on the MSKU3 method in terms of Pd, which is equal to 0.965 and 0.930, respectively. Also, in Figure 8(b) and the third column of Table 2, when N = 1000 samples, M = 2 SUs, Pf = 0.1, and at SNR = [-20dB, -20dB], the theoretical and practical performances of CSS based on the MSKU3 method are converged in terms of Pd and equal to 0.942 and 0.900, respectively. Furthermore, Figure 8(c) and the four columns of Table 2 confirm the convergence between the theoretical and practical performances of CSS based on the MSKU3 method for the same settings and at SNR = [-16 dB, -20 dB], where Pd is equal to 0.911 and 0.850, respectively. Finally, Figure 8 (d) and the five columns of Table 2 prove the convergence between the theoretical and practical performances of CSS based on the MSKU3 method for the same settings and at SNR = [-20 dB, -24 dB], where Pd is equal to 0.900 and 0.845, respectively. Even though the method that is developed is tailored to the noise channel, experimental and theoretical results match up. This is because of the idea of learning, which is achieved by using the unsupervised ML KMD.This indicates that the practical results that have been obtained under uncertain noise conditions and in real channel environments prove the validity of the theoretical methods that have been proposed for the CSS system.

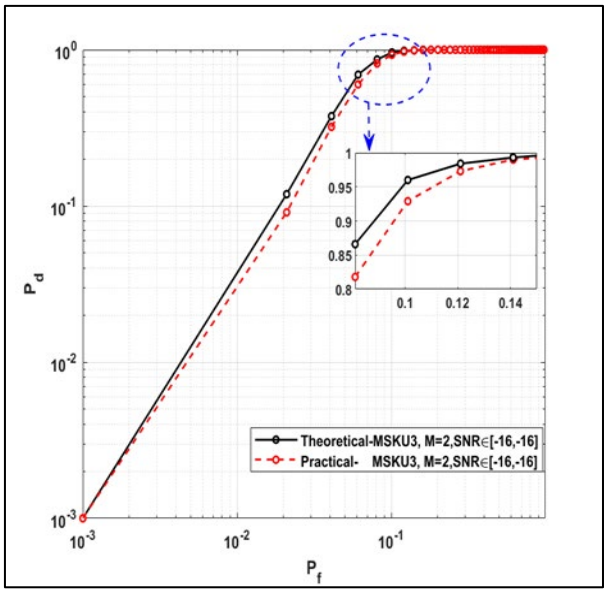

(a): M=2, SNR= [-16, -16]

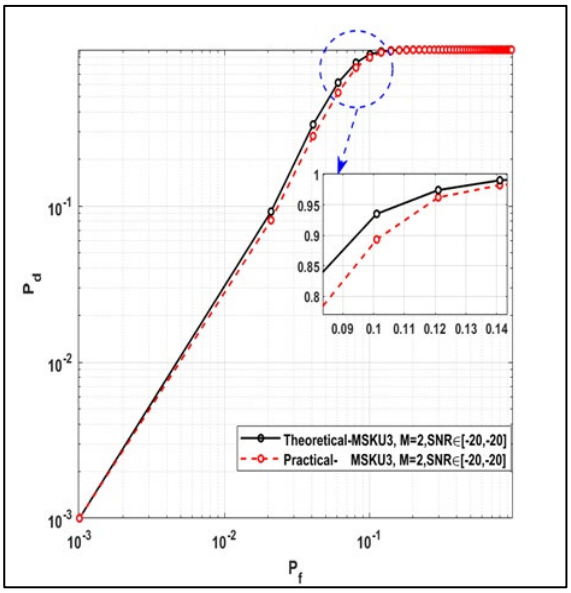

(b): M=2, SNR= [-20, -20]

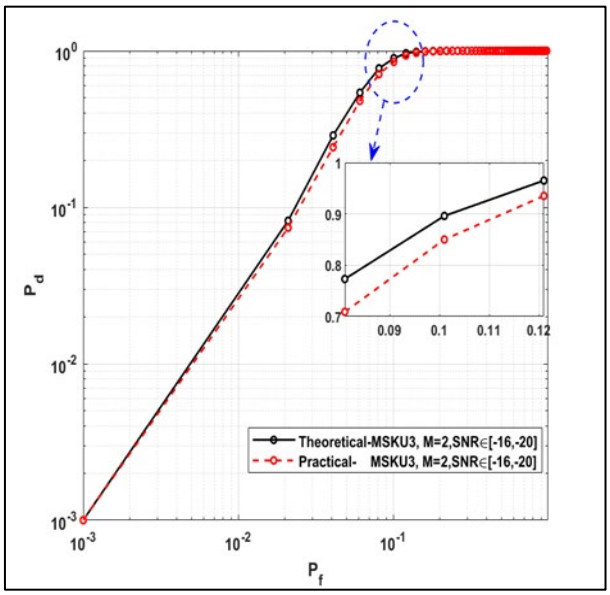

(c): M=2, SNR= [-16, -20]

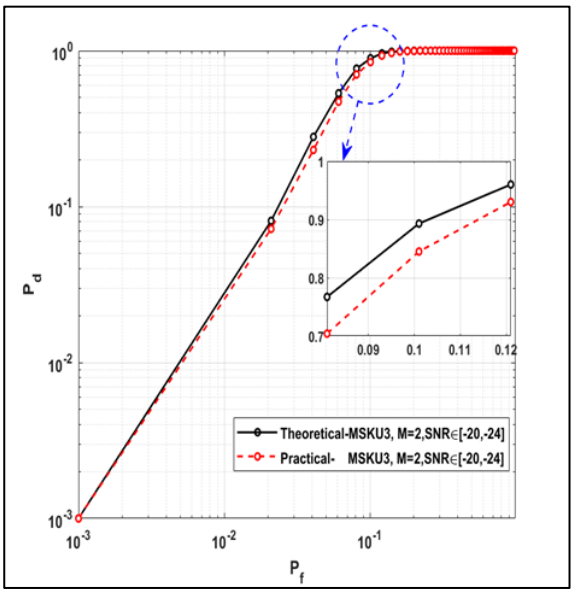

(d): M=2, SNR= [-20, -24]

Figure 8: Theoretical and practical results of CSS based on the MSKU3 method at different SNRs

Table 2: The P_d of the MSKU3 method with various SNR settings

Parameters / **MSKU3 Method**	**SNR = [-16dB, -16dB], $P_f = 0.1$**	**SNR = [-20dB, -20dB], $P_f = 0.1$**	**SNR = [-16dB, -20dB], $P_f = 0.1$**	**SNR = [-20dB, -24dB], $P_f = 0.1$**
Theoretical	0.965	0.942	0.911	0.900
Practical	0.930	0.900	0.850	0.845

4.3 Comparison of The Developed Method With Some Other Methods

As shown in Table 3, the key difference between our developed work [23] and other works [26,27,29] is that we use high-order moments (Sk and Ku-3) to build the DMF method and the unsupervised ML algorithm (KMD) for the trained classifier, whereas other works use features based on second-order moments such as CF, EF, and EF of RMT to derive a fixed threshold. Except work [31], which employed supervised ML algorithms such as Artificial Neural Networks (ANN), Support Vector Machines (SVM), decision trees (TREE), and K-Nearest Neighbors (KNN). On the other hand, in comparison to supervised ML algorithms, the unsupervised ML algorithm does not need previous knowledge about the actual PU channel. This would reduce the complexity of the proposed method and enhance the blind detection capability of the developed system [23]. In addition, deriving the threshold from the second-order moment is fixed, has a lot of computational complexity, and makes it hard to adapt to how the real channel of the PU signal changes over time [26,27,29]. Therefore, our proposed method has more benefits when it uses an unsupervised ML algorithm. For example, it avoids the computational complexity of fixed-threshold derivation and instead builds the classifier through the clustering process [23]. Moreover, the classifier construction is more prone to noise uncertainty, especially at low SNR, when using EF and RMT; on the contrary, when we use the classifier built on high-order moments (Sk and Ku-3), the proposed classifier is more immune to noise uncertainty.

Table 3: Comparison of the developed method with some other works

References / **Proposed Work** [23]	[1]	[26]	[27]	[29]	[31]
Developing the DMF method (MSKU3) based on the high-order moment, Sk, and access Ku.	Using a CF detector based on a second-order moment	Using an adaptive threshold energy detector based on second-order moments	Using the EF of RMT based on second-order moments	Using adaptive SS for CF and EF detectors based on a second-order moment	Using an EF detector based on second-order moments
KMD algorithm	No ML	No ML	No ML	No ML	Yes ML
GNU radio	GNU-Radio	GNU-Radio	unknown	GNU-Radio	MATLAB
RTL-SDR, PC, USRP N210	USRP N210, PC	USRP X310, PC	USRP RIO, PC	USRP, PC	Arduino, PC RTL-SDR
Lower complexity	High complexity	High complexity	High complexity	High complexity	Lower complexity

5. Conclusion

In this study, the hardware and software of the SDR platform have been used to verify the real-time sensing performance of a new MSKU3 method-based CSS scheme. Various SDR hardware and software are used to implement the developed system, such as RTL-SDR hardware as a receiver, GNU-Radio software to implement digital signal processing blocks of the proposed method, and USRP N210 hardware as a transmitter. The experimental results of sensing performance in terms of the probability of detection based on the SDR platform show the effectiveness of the proposed method in the current environment.

Acknowledgment

This research was implemented at the communication research center with help from the Ministry of Science and Technology in Baghdad, Iraq.

Author Contributions

Methodology Ali A. RADHI, Hanan A. R. Akkar, and Hikmat N. Abdullah; Software Ali A. RADHI; Formal Analysis Ali A. RADHI; Writing-Original Draft Preparation, Ali A. RADHI; Writing-Review & Editing, Ali A. RADHI, Hanan A. R. Akkar, and Hikmat N. Abdullah. “All authors have read and agreed to the published version of the manuscript.”

Funding

This research received no specific grant from any funding agency in the public, commercial, or not-for-profit sectors.

Data Availability Statement

Please, exclude this statement, the study did not report any data.

Conflicts of Interest

"The authors declare no conflict of interest."

References

[1] H. S. Abed, H. N. Abdullah, and M. A. Mahmood, Real-Time Hardware Implementation of Cyclostationary Spectrum Sensing for Various Modulation Types Using USRP, Int. Conf. Sp. Sci. Commun. Iconsp., 2021,2021, 54–59. https://doi.org/10.1109/IconSpace53224.2021.9768689

[2] C. Charan and R. Pandey, Cooperative spectrum sensing using eigenvalue-based double-threshold detection scheme for cognitive radio networks, Adv. Intell. Syst. Comput., 697 (2019) 189–199. https://doi.org/10.1007/978-981-13-1822-1_18

[3] R. Ouyang, T. Matsumura, K. Mizutani, and H. Harada, Software-Defined Radio-Based Evaluation Platform for Highly Mobile IEEE 802.22 System, IEEE Open J. Veh. Technol., 3 (2022) 167–177. https://doi.org/10.1109/OJVT.2022.3164461

[4] X. Tan, L. Zhou, H. Wang, Y. Sun, H. Zhao, and B. C. Seet, Cooperative Multi-Agent Reinforcement Learning Based Distributed Dynamic Spectrum Access in Cognitive Radio Networks, IEEE Int. Thi. J., 2022. https://doi.org/10.1109/JIOT.2022.3168296

[5] V. Ramani and S. K. Sharma, Cognitive radios: A survey on spectrum sensing, security and spectrum handoff, China Commun., 14 (2017) 185–208. https://doi.org/10.1109/CC.2017.8233660

[6] A. Ali and W. Hamouda, Advances on Spectrum Sensing for Cognitive Radio Networks: Theory and Applications, IEEE Commun. Surv. Tuts., 19 (2017) 1277–1304. https://doi.org/10.1109/COMST.2016.2631080

[7] H. Oh and H. Nam, Energy detection scheme in the presence of burst signals, IEEE Signal Process. Lett., vol. 26 (2019) 582–586. https://doi.org/10.1109/LSP.2019.2900165

[8] R. Shrestha and S. S. Telgote, A short sensing-time cyclostationary feature detection based spectrum sensor for cognitive radio network, Proc. - IEEE Int. Symp. Circuits Syst., 2020 (2020) 2–6. https://doi.org/10.1109/iscas45731.2020.9180415

[9] L. S. Cardoso, M. Debbah, P. Bianchi, and J. Najim, Cooperative spectrum sensing using random matrix theory, 3rd ISWPC 2008, Proc., 2008, 334–338. https://doi.org/10.1109/ISWPC.2008.4556225

[10] W. Zhao, H. Li, M. Jin, Y. Liu, and S. J. Yoo, Enhanced detection algorithms based on eigenvalues and energy in random matrix theory paradigm, IEEE Access, 8 (2020) 9457–9468. https://doi.org/10.1109/ACCESS.2020.2963935

[11] Z. Chen, H. Wang, Z. Sun, R. Sun, X. Ning, and L. Ren, Two Novel Spectrum Sensing Algorithms Based on Eigenvalue under Different Noise, ICSP, 2020 (2020)- 428–432. https://doi.org/10.1109/ICSP48669.2020.9321028

[12] Q. Chen, P. Wan, Y. Wang, J. Li, and Y. Xiao, Research on cognitive radio spectrum sensing method based on information geometry, Lect. Notes Comput. Sci., 10603 (2017) LNCS 554–564. https://doi.org/10.1007/978-3-319-68542-7_47

[13] F. Awin, N. Salout, and E. Abdel-Raheem, Combined fusion rules in cognitive radio networks using different threshold strategies, Appl. Sci., 9 (2019). https://doi.org/10.3390/app9235080

[14] R. Sarikhani and F. Keynia, Cooperative Spectrum Sensing Meets Machine Learning: Deep Reinforcement Learning Approach, IEEE Commun. Lett., 24 (2020) 1459–1462. https://doi.org/10.1109/LCOMM.2020.2984430

[15] S. Zhang, Y. Wang, J. Li, P. Wan, Y. Zhang, and N. Li, A cooperative spectrum sensing method based on information geometry and fuzzy c-means clustering algorithm, Eurasip J. Wirel. Commun. Netw., 2019 (2019). https://doi.org/10.1186/s13638-019-1338-z

[16] P. Shachi, K. R. Sudhindra, and M. N. Suma, Deep Learning for Cooperative Spectrum Sensing, in 2020 2nd PhD EDITS 2020, 2020, 20–21. https://doi.org/10.1109/PhDEDITS51180.2020.9315306

[17] A. Shirolkar and S. V. Sankpal, Deep Learning Based Performance of Cooperative Sensing in Cognitive Radio Network, 2021 2nd GCAT 2021, 2021. https://doi.org/10.1109/GCAT52182.2021.9587617

[18] V. Kumar, D. C. Kandpal, M. Jain, R. Gangopadhyay, and S. Debnath, K-mean clustering based cooperative spectrum sensing in generalized κ-μ Fading channels, 2016 22nd NCC 2016. https://doi.org/10.1109/NCC.2016.7561130

[19] Y. Cao and H. Pan, Energy-efficient cooperative spectrum sensing strategy for cognitive wireless sensor networks based on particle swarm optimization, IEEE Access, 8 (2020) 214707–214715. https://doi.org/10.1109/ACCESS.2020.3037707

[20] S. Zhang, Y. Wang, P. Wan, J. Zhuang, Y. Zhang, Y. Li, Clustering Algorithm-Based Data Fusion Scheme for Robust Cooperative Spectrum Sensing, IEEE Access.8 (2020) 5777–5786. https://doi.org/10.1109/ACCESS.2019.2963512

[21] H. A. R. Akkar, W. A. H. Hadi, I. H. Al-Dosari, S. M. Saadi, and A. I. Ali, Classification accuracy enhancement based machine learning models and transform analysis, Commun. - Sci. Lett. Univ. Zilina, 23 (2021) C44–C53. https://doi.org/10.26552/COM.C.2021.2.C44-C53

[22] A. A. Radhi, H. N. Abdullah, and H. A. R. Akkar, Denoised Jarque-Bera features-based K-Means algorithm for intelligent cooperative spectrum sensing, Digit. Signal Process. A Rev. J., 129 (2022) 1–15. https://doi.org/10.1016/j.dsp.2022.103659

[23] A. A. Radhi, H. A. R. Akkar, and H. N. Abdullah, Skewness and access kurtosis as denoised mixed features-based K-Medoids for cooperative spectrum sensing, Phys. Commun., 54 (2022) 1–15. https://doi.org/10.1016/j.phycom.2022.101831

[24] A. Martian, F. Lucian Chiper, O. Mohammed Khodayer Al-Dulaimi, M. Jalal Ahmad Al Sammarraie, C. Vladeanu, and I. Marghescu, Comparative Analysis of Software Defined Radio Platforms for Spectrum Sensing Applications, 2020 13th COMM 2020 Proc., 2020, 369–374. https://doi.org/10.1109/COMM48946.2020.9142024

[25] D. M. Molla, H. Badis, L. George, and M. Berbineau, Software Defined Radio Platforms for Wireless Technologies, IEEE Access, 10 (2022) 26203–26229. https://doi.org/10.1109/ACCESS.2022.3154364

[26] M. V. Lipski, S. Kompella, and R. M. Narayanan, Practical Implementation of Adaptive Threshold Energy Detection using Software Defined Radio, IEEE Trans. Aerosp. Electron. Syst., 57 (2021) 1227–1241. https://doi.org/10.1109/TAES.2020.3040059

[27] H. Ben Thameur and I. Dayoub, Real-Time In-Lab Test of Eigenvalue-Based Spectrum Sensing Using USRP RIO SDR Boards, IEEE Commun. Lett., 25 (2021) 1029–1032. https://doi.org/10.1109/LCOMM.2020.3037010

[28] A. Mate, K. H. Lee, and I. T. Lu, "Spectrum sensing based on time covariance matrix using GNU radio and USRP for cognitive radio," in 2011 IEEE LISAT 2011, 2–7. https://doi.org/10.1109/LISAT.2011.5784217

[29] A. Ivanov, A. Mihovska, K. Tonchev, and V. Poulkov, Real-time adaptive spectrum sensing for cyclostationary and energy detectors, IEEE Aerosp. Electron. Syst. Mag., 33 (2018) 20–33. https://doi.org/10.1109/MAES.2018.170098

[30] S. Majumder, Energy Detection Spectrum Sensing on RTL-SDR based IoT Platform, CICT 2018, 1–6, 2018, https://doi.org/10.1109/INFOCOMTECH.2018.8722360

[31] M. Saber, A. El Rharras, R. Saadane, A. Chehri, N. Hakem, and H. A. Kharraz, Spectrum sensing for smart embedded devices in cognitive networks using machine learning algorithms, Procedia Comput. Sci., 176 (2020) 2404–2413. https://doi.org/10.1016/j.procs.2020.09.311

[32] C. Gravelle and R. Zhou, SDR demonstration of signal classification in real-time using deep learning, GC Wkshps 2019 - Proc., 2019, https://doi.org/10.1109/GCWkshps45667.2019.9024661

[33] J. Zhuang, Y. Wang, P. Wan, S. Zhang, and Y. Zhang, Centralized spectrum sensing based on covariance matrix decomposition and particle swarm clustering, Phys. Commun., 46 (2021) 101322. https://doi.org/10.1016/j.phycom.2021.101322

[34] S. Zhang, Y. Wang, Y. Zhang, P. Wan, and J. Zhuang, A Novel Clustering Algorithm Based on Information Geometry for Cooperative Spectrum Sensing, IEEE Syst. J.,(2020) 1–10. https://doi.org/10.1109/jsyst.2020.3001407

[35] L. A. N. Man, S. Committee, and I. Computer, The Institute of Electrical and Electronics Engineering, Inc, Std. IEEE 802.22, (WRAN). 2020.

[36] J. Liang, M. L. Tang, and X. Zhao, Testing high-dimensional normality based on classical skewness and Kurtosis with a possible small sample size, Commun. Stat. - Theory Methods, 48 (20195719–5732. https://doi.org/10.1080/03610926.2018.1520882

[37] R. Kumar, R. K. D. Harishchandra, and D. V. P. Singh, Applications of Advanced Computing in Systems. Singapore: Springer Nature Singapore Pte Ltd, 2021.

[38] K. Vachhani and R. A. Mallari, Experimental study on wide band FM receiver using GNURadio and RTL-SDR, ICACCI. 2015, 2015, 1810–1814. https://doi.org/10.1109/ICACCI.2015.7275878

[39] J. Talukdar, B. Mehta, K. Aggrawal, and M. Kamani, Implementation of SNR estimation based energy detection on USRP and GNU radio for cognitive radio networks, Proc. 2017 Int. Conf. Wirel. Commun. Signal Process. Networking, 2018,2018,304–308. https://doi.org/10.1109/WiSPNET.2017.8299767

[40] X. Zhu, C. X. Wang, J. Huang, M. Chen, and H. Haas, A Novel 3D Non-Stationary Channel Model for 6G Indoor Visible Light Communication Systems, IEEE Trans. Wirel. Commun., 21 (2022) 1–16. https://doi.org/10.1109/TWC.2022.3165569